LAWRENCE
LIVERMORE
NATIONAL
LABORATORY

LLNL-TR-731680

Alternatives to argon for gas stopping volumes in the B194 neutron imager

D. L. Bleuel, S. Anderson, J. A. Caggiano, J. M. Hall, M. Johnson, A. Ratkiewicz, B. Rusnak

May 21, 2017

Disclaimer

This work performed under the auspices of the U.S. Department of Energy by Lawrence Livermore National Laboratory under Contract DE-AC52-07NA27344.

Alternatives to argon for gas stopping volumes in the B194 neutron imager

D. L. Bleuel, S. Anderson, J.A. Caggiano, J.M. Hall, M. Johnson, A. Ratkiewicz, B. Rusnak
May 17, 2017

In a recent experiment at Lawrence Berkeley National Laboratory, the ^{40}Ar(d,p)^{41}Ar excitation function between 3-7 MeV was measured, confirming a previous estimation that there may be an intolerable radiation dose from ^{41}Ar production by slowing to rest 6.74 MeV deuterons in the gas cell of the neutron imaging facility being constructed in B194. Gas alternatives to argon are considered, including helium, nitrogen (N_2), neon, sulfur hexafluoride (SF_6), krypton, and xenon, as well as high atomic number solid backings such as tantalum.

Helium

No deuteron or neutron reactions on helium produce radioactive byproducts. However, a high neutron production from ^{4}He(d,n)^{5}Li→α+p, ^{4}He(d,p)^{5}He→α+n and deuteron breakup may produce an unacceptable, low energy contamination of the otherwise quasi-monoenergetic imaging neutron beam. While neutron production experimental data is sparse, old, and highly uncertain in the literature, indications are that the cross sections for both (d,n) and (d,p)→α+n may be higher than that for D(d,n) at 7 MeV. Furthermore, the stopping range of 6.74 MeV deuterons in 3 atm helium gas is 70 cm, considerably longer than the current 14 cm gas stopping cell in which the beam would only lose 800 keV. Thus, the pressure would need to be significantly increased, the chamber extended, or a solid backing installed capable of absorbing the remaining heat load.

Nitrogen

The stopping range of 6.74 MeV deuterons in 3 atm of N_2 gas is about 12 cm. Thus, while the intended argon pressure of this cell is <2 atm, the existing 14 cm chamber would need to be filled with this increased pressure (equal to that of the deuterium gas) of nitrogen to stop the beam. From various reactions with deuterons, it is energetically possible to produce radioactive species, with half lives in parentheses, of ^{15}O (122 s), ^{14}C (5700 y), ^{13}N (10.0 m), ^{16}N (7.1 s) and ^{11}C (20.3 m). Of these, only ^{15}O is sufficiently long-lived and produced in enough abundance to present a potential radiation hazard outside the cave. A holding tank or an increased path length of piping may be used to hold the gas long enough for the 2-minute ^{15}O to decay, or the radioactive gas (most likely in the form of NO or N_2O) may be "scrubbed" with getters before exiting the cave. However, a major drawback to using nitrogen is, again, neutron production contaminating the primary imagining beam. The ^{14}N(d,n)^{15}O reaction cross section is 178 mb at 6.74 MeV, compared to the 91 mb cross section of D(d,n) at 7 MeV. Furthermore, it increases as the beam slows, with a peak cross section at 4 MeV of 220 mb, and remains substantial all the way down to ~2 MeV. The Q-value of this reaction is +5.07 MeV. Thus a spectrum of neutron energy is expected ranging from 0-13 MeV. While the exact thick-target, angular-dependent spectrum is not currently known, it is expected to be similar to that of measured deuteron reactions on other light-Z nuclei, with most of the 0° flux in a broad low-energy range up to ~5-6 MeV and a low-flux tail extending to the maximum energy.

Neon

The stopping range of 6.74 MeV deuterons in 3 atm of neon gas is about 20 cm, longer than the 14 cm depth of the existing chamber. Therefore, the pressure would have to be increased above 4.3 atm or the back of the chamber would have to dissipate heat from the remaining 2.86 MeV beam. The primary radioactive isotope production of concern is ^{18}F from ^{20}Ne(d,α) reactions. With a similar-magnitude cross section (~200 mb at 6.74 MeV) and half life (109 minutes) to ^{41}Ar production in argon, neon is not expected to be a significant improvement for radiation protection concerns unless the fluorine can be scrubbed from the gas before exiting the cave. Neutron production is expected to be high as well.

Sulfur Hexaflouride (SF_6)

Sulfer hexafluoride is an inert gas often used as an electrically-insulating gas in accelerator tanks and other industries. The only long-lived radioactive product from deuteron reactions on fluorine, is ^{18}F. Although, as previously noted, the expected hazard duration is similar to that of argon activation, the threshold of the ^{19}F(d,t)^{18}F reaction is 4.6 MeV and it was thought that production from 6.74 MeV deuterons stopping in SF_6 would be considerably lower than ^{41}Ar in argon. Unfortunately, the three experimental measurements of this cross section span two orders of magnitude, though all are significantly lower (<100 mb) at 6.74 MeV than ^{40}Ar(d,p)^{41}Ar, and drop quickly with decreasing energy to the threshold. More investigation is needed to compare the wildly-variant measurements in the literature. The primary hazardous isotopes from sulfur activation is from ^{30}P (2.5 min), ^{32}P (14.2 d), and ^{33}P (25.4 d). Of these, ^{30}P is likely the biggest concern, produced in ^{32}S(n,α) reactions. One experimentally-measured (Qaim et. al.) cross section is lower than 20 mb and dropping quickly with lower energy. Therefore, the radiation hazard of SF_6 is expected to be at least an order of magnitude lower than with argon. At a lower deuteron beam energy of 4 MeV (creating 7 MeV neutrons from thin-target D-D reactions), there would be very low dose rate concerns. However, as with all other low-Z target backings, neutron production is expected to be of high concern.

Krypton

The ideal stopping target is one high enough in Z that the Coulomb barrier is significantly higher than the 6.74 MeV beam energy, inhibiting both activation and neutron production. Using the charge radius of 2.1415 fm for a deuteron and $1.25A^{1/3}$ fm for heavier nuclei, the center-of-mass Coloumb barrier of krypton (Z=36) is almost exactly that of the beam energy. Thus, while deuteron reaction cross sections are lower than for argon, they are not negligible. Natural krypton has eight stable isotopes and while neutron production on each is expected to be somewhat lower, reactions on all of them will produce a great variety of radioactive products. While the dose rate from these products is estimated to be orders of magnitude lower than that from argon activation, many of these products have half lives on order of days or months and long-term use of the facility will slowly build up this radiation hazard which will not decay for years.

Xenon

As with krypton, xenon has a large number (9) of stable isotopes, deuteron reactions on which can create a medley of long-lived radioactive productions. However, the Coulomb barrier for deuterons on xenon (Z=54) is over 9 MeV, above the 6.74 MeV deuteron energy, making it a better candidate for a gas stopping medium with lower activation and neutron production potential. However, while lower, it's neutron and radioactive isotope production can still not be neglected. Unfortunately, xenon, which can condense into a liquid phase when compressed, is incompatible with the high flow rate needed.

Tantalum, Tungsten, Rhenium (or other high-Z solid backing)

The high current (300 uA average, 25 mA peak) and energy (6.74 MeV) of the deuteron beam produces 2 kW of average power with 169 kW peak power spikes during each beam pulse. This heat load is extremely difficult to dissipate in solid targets without melting the material. High-Z materials minimize activation and neutron production, in particular elements with higher charge than neodymium (Z=60), where the deuteron Coulomb barrier is greater than ~3 MeV above the beam energy. Furthermore, the deuteron reaction activation products of a solid target are fixed in place and do not pose an external hazard as gases circulating outside the facility. However, the build-up of these activated products can make maintenance of the target more problematic. Tantalum (Z=73, T_{melt}=3017 °C, thermal conductivity=57 W/m-K) or tungsten (Z=74, T_{melt} =3422 °C, thermal conductivity=174 W/m-K) are natural options. Rhenium (Z=75, T_{melt}=3186 °C, thermal conductivity=48 W/m-K), while considerably more expensive, has comparably favorable properties, is more ductile when annealed, and can be carburized to increase its emissivity.

TZM (Solid)

Another solid backing material considered is "TZM," a Ti/Zr/Mo alloy consisting primarily (99%) of molybdenum (Z=42). The short term (hours to days) activation from deuteron reactions is expected to be an order of magnitude higher than for higher-Z tantalum or tungsten, but long term activation (months) is expected to be lower. Unfortunately, although the Coulomb barrier for deuterons on molybdenum exceeds the beam energy, the expected neutron production cross sections are still significant. For minimal neutron contamination, a higher-Z target is desired.

Conclusion

Unfortunately, there is no perfect material yet identified as a deuteron stopping medium with properties of low long-lived activation, low neutron production, sufficient stopping power within the 14 cm gas chamber, suitable gas compressibility, and sufficient heat transfer capabilities. These characteristics for each candidate is pictorially summarized in the Chart below, with red boxes indicating probable intolerable properties. The yellow box indicates that the activation issues for nitrogen may be mitigated while the orange box for krypton differentiates its lower-dose, long-lived (months) issues versus argon's high-dose, short-lived (hours) issue:

	Ar	He	N_2	Ne	SF_6	Kr	Xe	Ta/W	TZM
Activation									
Neutron production									
Stops beam <14 cm @ 3 atm									
Gas compressibility									
Heat transfer w/o melting									

Potentially, the most promising candidate is a high-Z material such as tantalum or tungsten if a design can be implemented that resists melting or ablation.

Appendix 1: TENDL-weighted cross sections

For quick comparison of the approximate neutron and isotope production for all the considered target backing options, spectrum-averaged, neutron-emitting, theoretical cross sections, <σ>, from TENDL were calculated for a deuteron beam spectrum representative of stopping from 7 MeV in a thick argon target and tabulated in Appendices 2 (neutrons) and 3 (isotopes). This stopping deuteron spectrum used is shown:

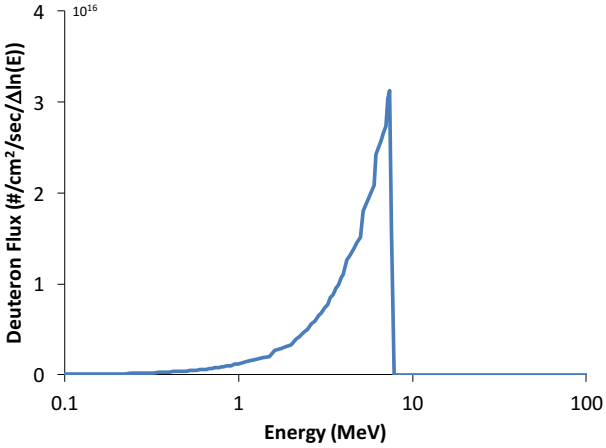

These spectrum-averaged cross sections for neutron production on thick targets considered in this report, as well as some light-Z neutron source candidates (^{9}Be, ^{10,11}B, ^{12,13}C), are depicted versus the thin-target (7 MeV) cross section for D(d,n):

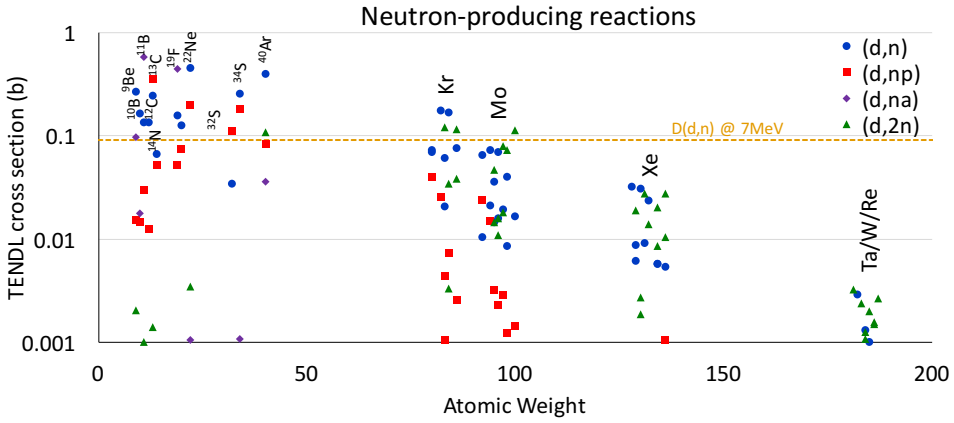

Radioactive isotope production for select reactions with a high potential of presenting a dose hazard are similarly shown, grouped by color/symbol according to half life (between 10s and 100y):

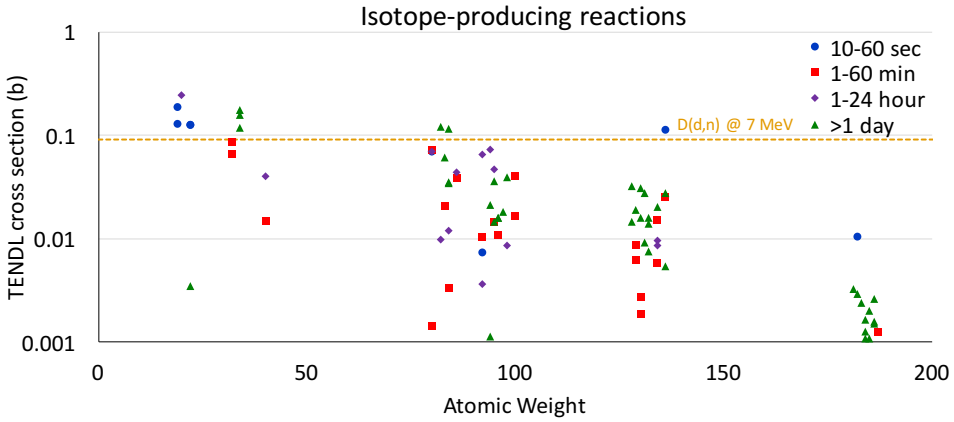

Appendix 2: Neutron production cross sections

Tabulated are spectrum-weighted cross sections, described in Appendix 1, for neutron-producing reactions for materials considered in this report. Only cross sections greater than 10 mb are included, for isotopes with greater than 1% natural abundance. Note that these 4π-integrated cross sections do not necessarily represent 0° neutron yield and these theoretical cross sections often do not match experimental values indicated earlier in this report. Therefore, this table and charts in Appendix 1 only serve as a rough guide to overall production.

Reaction	Abundance	<σ> (mb)	Q (MeV)
N14(d,np)N14	99.4%	53	-2.22
N14(d,n)O15		68	5.07
F19(d,na)O16	100%	443	-3.90
F19(d,np)F19		52	-2.22
F19(d,n)Ne20		157	10.62
Ne20(d,np)Ne20	90.5%	75	-2.22
Ne20(d,n)Na21		126	0.21
Ne22(d,np)Ne22	9.25%	201	-2.22
Ne22(d,n)Na23		457	6.57
S32(d,np)S32	95.0%	111	-2.22
S32(d,n)Cl33		35	0.05
S34(d,np)S34	4.25%	184	-2.22
S34(d,n)Cl35		259	4.15
Ar40(d,na)Cl37	99.6%	36	-0.64
Ar40(d,np)Ar40		83	-2.22
Ar40(d,2n)K40		108	-4.51
Ar40(d,n)K41		396	5.58
Kr80(d,np)Kr80	2.29%	40	-2.22
Kr80(d,n)Rb81		70	2.63
Kr80(d,n)Rb81m		73	3.49
Kr82(d,np)Kr82	11.6%	26	-2.22
Kr82(d,n)Rb83		175	3.54
Kr83(d,2n)Rb83	11.5%	121	-3.93
Kr83(d,n)Rb84		62	4.83
Kr83(d,n)Rb84m		21	5.29
Kr84(d,2n)Rb84	57.0%	35	-5.69
Kr84(d,n)Rb85		168	4.79
Kr86(d,2n)Rb86	17.3%	115	-3.53
Kr86(d,2n)Rb86m		38	-2.97
Kr86(d,n)Rb87		76	6.40
Mo92(d,np)Mo92	14.5%	24	-2.22
Mo92(d,n)Tc93		65	1.86
Mo92(d,n)Tc93m		11	2.25
Mo94(d,np)Mo94	9.15%	15	-2.22
Mo94(d,n)Tc95		73	2.67
Mo94(d,n)Tc95m		21	2.71
Mo95(d,2n)Tc95	15.8%	47	-4.70
Mo95(d,2n)Tc95m		15	-4.66
Mo95(d,n)Tc96		36	3.17
Mo95(d,n)Tc96m		15	3.20
Mo96(d,2n)Tc96	16.7%	16	-5.98
Mo96(d,2n)Tc96m		11	-5.95
Mo96(d,n)Tc97		71	3.49
Mo96(d,n)Tc97m		16	3.59
Mo97(d,2n)Tc97	9.60%	80	-3.33
Mo97(d,2n)Tc97m		18	-3.23
Mo97(d,n)Tc98		20	3.95
Mo98(d,2n)Tc98	24.4%	74	-4.69
Mo98(d,n)Tc99		41	4.28
Mo100(d,2n)Tc100	9.82%	115	-3.18
Mo100(d,n)Tc101		17	5.22
Xe128(d,n)Cs129	1.91%	32	2.70
Xe129(d,2n)Cs129	26.4%	19	-4.20
Xe130(d,n)Cs131	4.07%	31	3.24
Xe131(d,2n)Cs131	21.2%	28	-3.36
Xe132(d,2n)Cs132	26.9%	14	3.80
Xe132(d,n)Cs133		24	3.86
Xe134(d,2n)Cs134	10.4%	21	-5.13
Xe136(d,2n)Cs136	8.86%	28	-3.10
Xe136(d,2n)Cs136m		11	-2.58

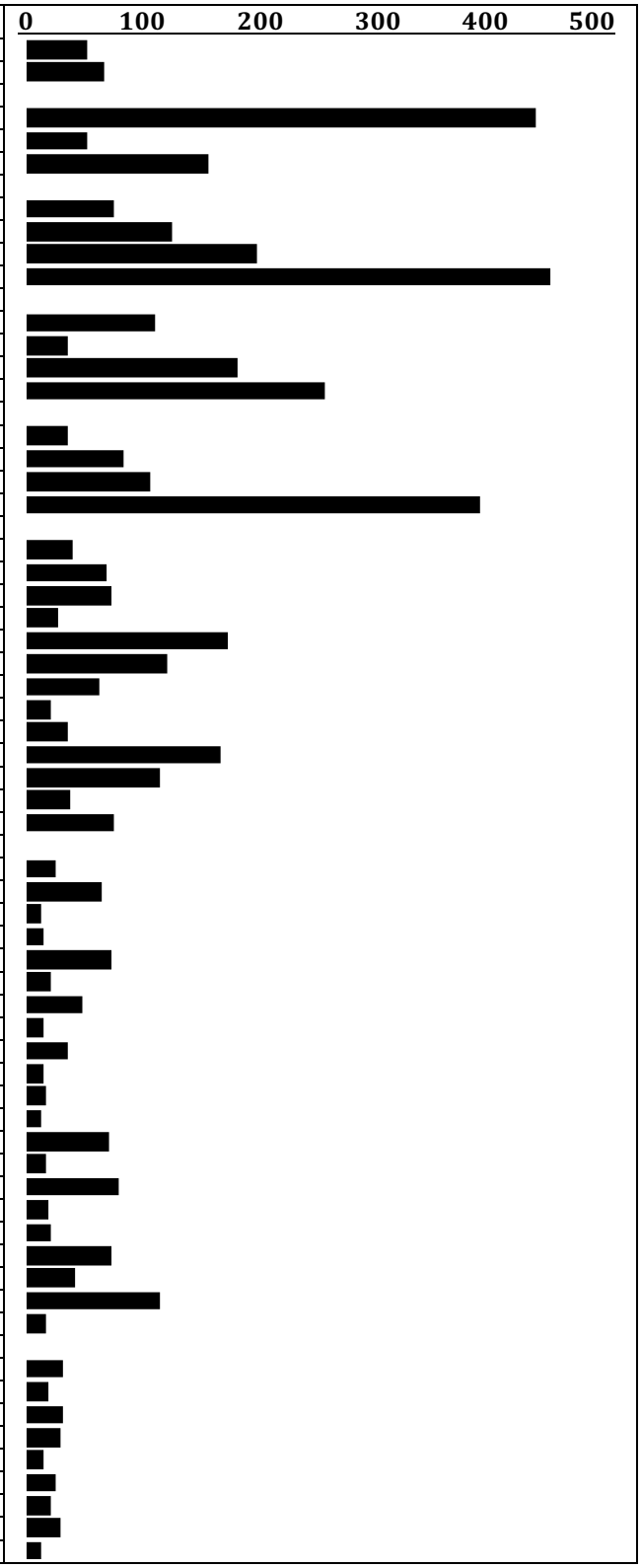

Appendix 3: Radioactive isotope production cross sections

Again for quick comparison, similar spectrum-weighted theoretical cross sections from TENDL, described in Appendix 1, are shown for reactions which generate high-dose-risk radioactive isotopes with half lives greater than 10 seconds and less than 100 years. Only cross sections greater than 10 mb are included, for isotopes with greater than 1% natural abundance. No consideration is given for decay chains; thus short-lived species that produce longer-lived products may be improperly unrepresented.

Reaction	Abundance	<σ> (mb)	$T_{1/2}$
N14(d,n)O15	99.4%	68	2.0 m
F19(d,p)F20	100%	129	11.1 s
Ne20(d,a)F18	90.5%	245	1.8 h
Ne20(d,n)Na21		126	22.5 s
Ne22(d,a)F20	9.25%	127	11.1 s
Ne22(d,p)Ne23		71	37.2 s
S32(d,a)P30	95.0%	86	2.5 m
S34(d,a)P32	4.25%	120	14.3 d
S34(d,p)S35		157	87.4 d
Ar40(d,a)Cl38	99.6%	15	37.2 m
Ar40(d,p)Ar41		41	1.8 h
Kr80(d,n)Rb81	2.29%	70	4.6 h
Kr80(d,n)Rb81m		73	30.5 m
Kr82(d,n)Rb83	11.6%	175	86.2 d
Kr83(d,2n)Rb83	11.5%	121	86.2 d
Kr83(d,n)Rb84		62	32.8 d
Kr83(d,n)Rb84m		21	20.3 m
Kr84(d,p)Kr85	57.0%	35	3927.1 d
Kr84(d,p)Kr85m		12	4.5 h
Kr84(d,2n)Rb84		35	32.8 d
Kr86(d,p)Kr87	17.3%	45	1.3 h
Kr86(d,2n)Rb86		115	18.6 d
Kr86(d,2n)Rb86m		38	1.0 m
Mo92(d,n)Tc93	14.5%	65	2.8 h
Mo92(d,n)Tc93m		11	43.5 m
Mo94(d,n)Tc95	9.15%	73	20.0 h
Mo94(d,n)Tc95m		21	61.0 d
Mo95(d,2n)Tc95	15.8%	47	20.0 h
Mo95(d,2n)Tc95m		15	61.0 d
Mo95(d,n)Tc96		36	4.3 d
Mo95(d,n)Tc96m		15	51.5 m
Mo96(d,2n)Tc96	16.7%	16	4.3 d
Mo96(d,2n)Tc96m		11	51.5 m
Mo96(d,n)Tc97m		16	91.0 d
Mo97(d,2n)Tc97m	9.60%	18	91.0 d
Mo98(d,p)Mo99	24.4%	40	2.7 d
Mo100(d,p)Mo101	9.82%	40	14.6 m
Mo100(d,2n)Tc100		115	15.5 s
Mo100(d,n)Tc101		17	14.0 m
Xe128(d,p)Xe129m	1.91%	15	8.9 d
Xe128(d,n)Cs129		32	1.3 d
Xe129(d,2n)Cs129	26.4%	19	1.3 d
Xe130(d,p)Xe131m	4.07%	16	11.8 d
Xe130(d,n)Cs131		31	9.7 d
Xe131(d,2n)Cs131	21.2%	28	9.7 d
Xe132(d,p)Xe133m	26.9%	16	2.2 d
Xe132(d,2n)Cs132		14	6.5 d
Xe134(d,p)Xe135m	10.4%	15	15.3 m
Xe134(d,2n)Cs134		21	754.3 d
Xe136(d,p)Xe137	8.86%	26	3.8 m
Xe136(d,2n)Cs136		28	13.0 d
Xe136(d,2n)Cs136m		11	17.5 s